IEEE Access
Multidisciplinary ⋮ Rapid Review ⋮ Open Access Journal

Date of publication xxxx 00, 0000, date of current version xxxx 00, 0000.

Digital Object Identifier 10.1109/ACCESS.2020.Doi Number

Entanglement Assisted Radars with Transmitter Side Optical Phase Conjugation and Classical Coherent Detection

IVAN B. DJORDJEVIC, (Fellow, IEEE)
University of Arizona, Department of Electrical and Computer Engineering, 1230 E. Speedway Blvd., Tucson, AZ 85721, USA

Corresponding author: Ivan B. Djordjevic (e-mail: ivan@email.arizona.edu).

ABSTRACT Entanglement is a unique quantum information processing feature. With the help of entanglement we can build quantum sensors whose sensitivity is better than that of classical sensors. In this paper we are concerned with the entanglement assisted (EA) bistatic quantum radar applications. By employing the optical phase conjugation (OPC) on transmitter side and classical coherent detection on receiver side we show that the detection probability of the proposed EA target detection scheme is significantly better than that of corresponding classical and coherent states-based quantum detection schemes. The proposed EA target detection scheme is evaluated by modelling the radar return channel as the lossy and noisy Bosonic channel and assuming imperfect distribution of entanglement over the idler channel.

INDEX TERMS Entanglement, Radars, Quantum sensing, Quantum radars, Entanglement assisted quantum radars.

I. INTRODUCTION

The entanglement is a unique quantum information processing (QIP) attribute [1]-[4]. With the help of entanglement we can: (1) beat the sensitivity of classical sensors [1],[5],[6], (2) enable communication networks with unconditional security [1],[2],[4],[7], and (3) communicate at rates above the classical channel capacity [8]-[10]. By distributing the entanglement at a distance, we can interconnect various quantum devices and modules thus enabling secure distributed quantum computing [11] and distributed quantum sensing [1],[5].

The key motivation behind the quantum radar studies is to beat the quantum limit of classical sensors [12]. The potential advantages of quantum radars compared to the classical radars can be summarized as follows: better receiver sensitivity, better target detection probability in a low signal-to-noise ratio (SNR) regime, improved penetration through clouds and fog when microwave photons are used, better resilience to jamming, improved synthetic-aperture radar imaging quality, the quantum radar signals are more difficult to detect compared to classical counterparts, and quantum radars have higher cross-section (as shown in [12]), to mention few. Unfortunately, they are significantly more challenging to implement. Two popular quantum radar designs are: (i) interferometric quantum radar, with the concept being very similar to the quantum interferometry, and (ii) the quantum radar employing the quantum illumination sensing concept proposed by Lloyd [13]-[21]. For classification of different quantum radar techniques an interested reader is referred to [16],[18]. For additional details on quantum illumination we refer the reader to a tutorial paper by Shapiro [14]. The quantum illumination concept at microwave frequencies was experimentally demonstrated in [21].

In this paper, we are concerned with the entanglement assisted (EA) bistatic quantum radar detection, whose operational principle is illustrated in Fig. 1.

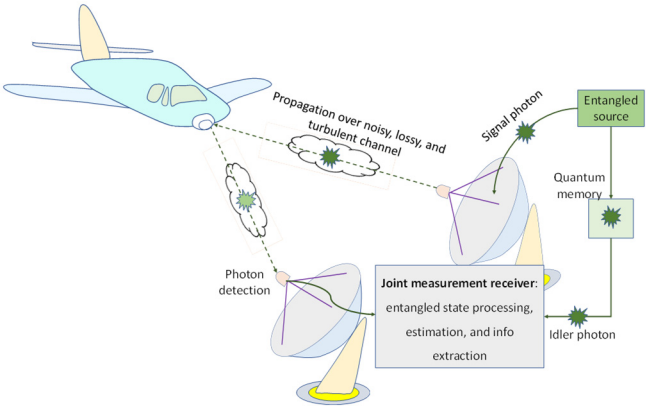

FIGURE 1. **Illustration of the EA bistatic quantum radar concept.**

The entangled source generates an entangled pair of photons, the signal and idler photons. The idler photon is kept in the quantum memory of the receiver, while the signal photon is transmitted over noisy, lossy, and atmospheric turbulent channel towards the target. The reflected photon is detected by the radar and quantum correlation is exploited to improve the target detection probability.

To improve the target detection probability we propose to employ the optical phase conjugation (OPC) on transmitter side and classical coherent detection on receiver side. We show that the proposed EA target detection scheme significantly outperforms coherent states-based quantum detection and classical counterparts. We evaluate the proposed EA target detection scheme by modelling the transmitter-target-receiver (main) channel as the lossy and noisy Bosonic channel and assuming that the distribution of entanglement over the idler channel is imperfect.

In the rest of this section the organization of the paper is provided. The EA radar concept is introduced in Sec. II. Both signal and idler channels are modeled as lossy and noisy Bosonic channels. The proposed EA radar scheme, employing the OPC on transmitter side and coherent detection on receiver side, is described in Sec. III. In Sec. IV we evaluate the detection probability performances of the proposed EA target detection scheme and compare it against coherent states-based quantum detection schemes. The concluding remarks are provided in the last section (Sec. V).

II. ENTANGLEMENT ASSISTED QUANTUM RADARS

In this section, we describe the entanglement assisted target detection by employing the Gaussian states generated through the continuous-wave spontaneous parametric down conversion (SPDC) process. The SPDC-based entangled source is broadband source containing $D=T_{meas}B$ i.i.d. signal-idler photon pairs, where T_{meas} is the measurement interval and B is the phase-matching SPDC bandwidth. Each signal-idler photons pair, with corresponding signal and idler creation operators denoted by $\hat{a}_s^\dagger$ and $\hat{a}_i^\dagger$, respectively, is in fact a two-mode squeezed vacuum (TMSV) state whose representation in Fock basis is given by:

$$|\psi\rangle_{s,i} = \frac{1}{\sqrt{N_s+1}} \sum_{n=0}^{\infty} \left(\frac{N_s}{N_s+1} \right)^{n/2} |n\rangle_s |n\rangle_i, \qquad (1)$$

where $N_s = \langle \hat{a}_s^\dagger \hat{a}_s \rangle = \langle \hat{a}_i^\dagger \hat{a}_i \rangle$ denotes the mean photon number per mode. The signal-idler entanglement is specified by the phase-sensitive cross-correlation (PSCC) coefficient $\langle \hat{a}_s \hat{a}_i \rangle = \sqrt{N_s(N_s+1)}$, which can be interpreted as the quantum limit. The TMSV state is a pure maximally entangled zero-mean Gaussian state with the following Wigner covariance matrix:

$$\mathbf{\Sigma}_{TMSV} = \begin{bmatrix} (2N_s+1)\mathbf{1} & 2\sqrt{N_s(N_s+1)}\mathbf{Z} \\ 2\sqrt{N_s(N_s+1)}\mathbf{Z} & (2N_s+1)\mathbf{1} \end{bmatrix}, \qquad (2)$$

where $\mathbf{Z}$=diag(1,–1) denotes the Pauli Z-matrix and $\mathbf{1}$ denotes the identity matrix. Evidently, in the low-brightness regime N_s<<1, the PSCC is $\langle \hat{a}_s \hat{a}_i \rangle \approx \sqrt{N_s}$ that is much larger than the corresponding classical limit N_s. As described earlier, by going back to Fig. 1, the entangled source is used on transmitter side to generate quantum correlated signal photon (probe) and idler photon (local reference). The signal photon is transmitted over noisy, lossy, and atmospheric turbulent channel towards the target. The reflected photon (also known as the radar return) is detected by the radar's receiver, and quantum correlation between radar return and retained reference (idler photon) is exploited to improve the receiver sensitivity. The interaction between the probe (signal) photon and the target can be described by a beam splitter of transmissivity T. Therefore, we can model the radar transmitter-target-radar receiver (main) channel as a lossy thermal Bosonic channel

$$\hat{a}_{\mathrm{Rx}}(\varphi) = \sqrt{T} e^{-j\varphi} \hat{a}_s + \sqrt{1-T}\,\hat{a}_b, \qquad (3)$$

where $\hat{a}_b$ is a background (thermal) state with the mean photon number being $(1-T)\langle \hat{a}_b^\dagger \hat{a}_b \rangle = N_b$. With φ we denoted signal-mode phase shift introduced by the target and channel. The idler-mode channel is assumed to be imperfect and can also be described by the lossy and noisy Bosonic channel

$$\hat{a}_{\mathrm{Rx,\,idler}} = \sqrt{T_i}\,\hat{a}_i + \sqrt{1-T_i}\,\hat{a}_{bi}, \qquad (4)$$

where T_i is transmissivity of the idler channel and $\hat{a}_{bi}$ is the annihilation operator of the background (thermal) mode of the idler channel with the mean photon number being $(1-T_i)\langle \hat{a}_{bi}^\dagger \hat{a}_{bi} \rangle = N_{bi}$. The radar returned probe and retained reference (stored idler) can be described by the following covariance matrix:

$$\mathbf{\Sigma}_t = \begin{bmatrix} (2N_s+1)\mathbf{1} & 2\sqrt{TT_iN_s(N_s+1)}\mathbf{Z}\delta_{1t} \\ 2\sqrt{TT_iN_s(N_s+1)}\mathbf{Z}\delta_{1t} & (2N_s'+1)\mathbf{1} \end{bmatrix}, \qquad (5)$$

where $N_s' = (T_iN_s + N_{bi})T + N_b$. We use t to denote the target indicator, wherein the absence of the target is denoted by t=0 and in this case the return signal does not contain the probe, just the background noise, and the covariance matrix is diagonal. The presence of the target is denoted by t=1 and antidiagonal terms, representing the quantum correlation between the signal and idler, are non-zero in this case.

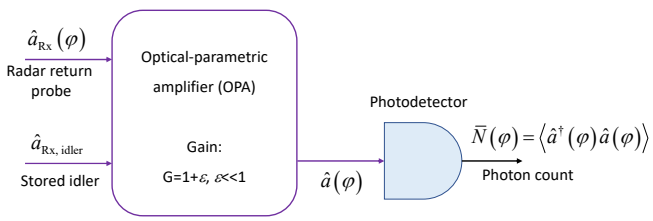

FIGURE 2. The operation principle of the optical-parametric amplifier (OPA)-based receiver.

The joint measurement receiver may use the optical parametric amplifier (OPA), shown in Fig. 2, with a low gain $G-1=\varepsilon<<1$, to obtain:

$$\hat{a}(\varphi)=\sqrt{G}\ \hat{a}_{\text{Rx, idler}}+\sqrt{G-1}\ \hat{a}_{\text{Rx}}^{\dagger}(\varphi) \tag{6}$$

for each signal-idler pair of a given mode. The direct detection of the OPA has the following mean photon number $\bar{N}(\varphi)=\left\langle \hat{a}^{\dagger}(\varphi)\hat{a}(\varphi)\right\rangle$. The authors have shown in [23] that with the help of OPA, the entanglement assisted receiver for ideal distribution of the idler (T_i=1) provides maximum 3 dB improvement over corresponding classical receiver. However, in the presence of experimental imperfections the improvement was reduced down to 1 dB.

Given that the OPC receiver has better sensitivity than the OPA receiver as shown in [5],[9],[10], here we study an EA target detection scheme employing the OPC. Moreover, the EA communication employing the OPC-based receiver has been experimentally demonstrated in [22]. The key difference of our target detection scheme is that the OPC operation is performed on transmitter side, rather than receiver side in [5],[22], while classical coherent detection is applied on receiver side, with details provided in incoming section. Furthermore, the performances in [5] were evaluated in terms of probability of error not the detection probability that is more relevant in radar applications. Additionally, the closed-form expression for the detection probability is derived here. Finally, we assume that the distribution of entanglement is not perfect. By moving the OPC operation to transmitter side we can: (i) extend the transmission distance because the low-brightness regime can be redefined as $TN_s<<1$, (ii) integrate the EA transmitter with modulator on the same chip, and (iii) reduce the complexity for multistatic radar applications because the OPC will be performed only once on transmitter side as opposed to performing the OPC on receiver side given that each receiver will need the nonlinear device to perform the OPC. In principle, the maximum entangled states are not needed to achieve the quantum advantage as shown in [17]. Various coherent states-based quantum detection schemes outperform the classical target detection as shown in Sec. IV. However, by using the entangled sates additional improvements are possible. Given that the TMSV states can straightforwardly be generated through the SPDC process and corresponding theory is well developed, we prefer to use the TMSV states in the EA target detection scheme studied here.

III. ENTANGLEMENT ASSISTED RADAR DETECTION WITH TRANSMITTER SIDE OPTICAL PHASE CONJUGATION AND COHERENT DETECTION

In this section we describe our proposed entanglement assisted radar detection concept, which is inspired by our recently proposed entanglement assisted communication system [10]. The integrated entanglement assisted transmitter, based on $LiNbO_3$ technology, performing optical phase conjugation on transmitter side, is shown in Fig. 3. The phase or I/Q modulator is optional. In Figure 3 we use s to denote a signal constellation point imposed by either phase modulator or I/Q modulator. For instance, for M-ary PSK we have that $s=\exp(\mathrm{j}\theta_m)$.

To perform the OPC through the difference frequency generation (DFG) we employ the periodically poled $LiNbO_3$ (PPLN) waveguide. The SPDC concept is employed in the first PPLN waveguide to generate signal-idler photon pairs, which get separated by Y-junction. The DFG interaction of the pump photon ω_p and signal photon ω_s takes place in the second PPLN to generate the phase-conjugated photon at $\omega_{OPC}=\omega_p-\omega_s$. As an illustrative example, assuming that the strong pump laser diode at λ_p=780 nm is used, through the SPDC process the following signal-idler pair can be generated: the signal photon at wavelength λ_s=1585.8 nm and the idler photon at wavelength λ_i=1535 nm. In the OPC PPLN waveguide the signal photon get interacted with the pump photon through the DFG process to obtain the phase-conjugated (PC) signal photon at wavelength $\lambda_{s,PC}=1/(1/\lambda_p-1/\lambda_s)$=1530 nm, which is the same as the idler photon wavelength.

Therefore, by performing the OPC on transmitter side, conventional-classical balanced coherent detection receiver is applicable on receiver side, with one such receiver provided in Fig. 4. Clearly, the OPC radar return probe and idler modes are mixed on balanced beam splitter, followed by two photodetectors. The idler mode serves as a local laser signal for homodyne coherent detection.

For the transmit side OPC, the main channel model becomes

$$\hat{a}_{\text{Rx}}(\varphi)=\sqrt{T}e^{-j\varphi}\hat{a}_s^{\dagger}+\sqrt{1-T}\hat{a}_b, \tag{7.1}$$

wherein the overall phase φ is composed of three components:

$$\varphi=\theta_m+\vartheta+\phi, \tag{7.2}$$

where θ_m is the modulation phase (when M-ary PSK is used), while ϑ denotes the phase-shift introduced by the target and assuming that transmitter and receiver are in close proximity it is related to the distance d from the target by $\vartheta=2kd$, with k being the wave number related to the wavelength λ by $k=2\pi/\lambda$. Finally, ϕ is the random phase shift introduced by the channel. The sequence encoded on transmitter side is used as a pilot sequence for estimation and cancelation of the random phase shift.

The operation principle of the entanglement assisted bistatic radar, provided in Fig. 1, is already described in previous section.

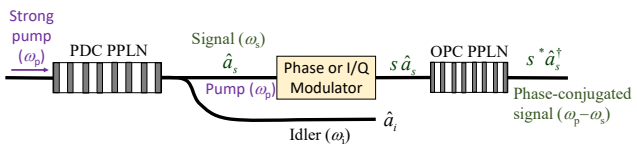

FIGURE 3. **$LiNbO_3$ technology-based integrated entanglement assisted transmitter with OPC implemented on transmitter side. PDC: parametric down conversion, OPC: optical phase-conjugation, PPLN: periodically poled $LiNbO_3$ waveguide.**

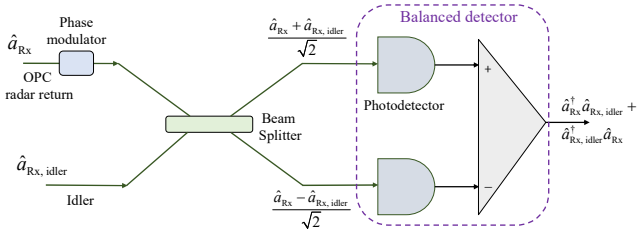

FIGURE 4. Entanglement assisted homodyne balanced detection receiver. The phase modulator is used to detect either in-phase or quadrature component of the OPC signal. Photodiode responsivity is set to 1 A/W.

The balanced detector (BD) photocurrent operator (assuming that the photodiode responsivity is 1 A/W) is given by:

$$\hat{i}_{BD} = \hat{a}^{\dagger}_{Rx}\hat{a}_{\mathrm{Rx,idler}} + \hat{a}^{\dagger}_{\mathrm{Rx,idler}}\hat{a}_{Rx}. \tag{8}$$

For the receive side phase modulator shift of Δφ=0 rad (see Fig. 4), in the presence of the target, we obtain the following BD photocurrent operator expectation:

$$\left\langle \hat{i}_{BD} \right\rangle = 2\sqrt{T_i T N_s \left(N_s+1\right)}\cos\varphi, \tag{9}$$

On the other hand, for the receive side phase modulator shift of Δφ=−π/2 rad, in the presence of target, we obtain the following BD photocurrent operator expectation:

$$\left\langle \hat{i}_{BD} \right\rangle = 2\sqrt{T_i T N_s \left(N_s+1\right)}\sin\varphi. \tag{10}$$

Both in-phase and quadrature component are needed if we want to determine the exact phase-shift and the target range.

For the receive side phase modulator shift of Δφ=0 rad, the variance of the BD photocurrent operator, defined as $\mathrm{Var}\left(\hat{i}_{BD}\right) = \left\langle \hat{i}_{BD}{}^2 \right\rangle - \left\langle \hat{i}_{BD} \right\rangle^2$, will be:

$$\begin{aligned}\mathrm{Var}\left(\hat{i}_{BD}\right) &= N_i N_s' + \left(N_i+1\right)\left(N_s'+1\right) \\ &\quad + 2N_s T T_i (N_s+1)\left[\cos\left(2\varphi\right) - 2\cos^2\varphi\right],\end{aligned} \tag{11}$$

where $N_s' = (T_i N_s + N_{bi})T + N_b$.

In the absence of the target, the BD photocurrent operator expectation is zero, while the corresponding variance is:

$$\begin{aligned}\mathrm{Var}\left(\hat{i}_{BD}^{t=0}\right) &= N_i N_b + \left(N_i+1\right)\left(N_b+1\right) \\ &= N_s N_b + \left(N_s+1\right)\left(N_b+1\right),\end{aligned} \tag{12}$$

where we used the fact that N_i=N_s.

Given that in the target detection problem *a priori* probabilities are not known we apply the Neyman-Pearson criterion [24],[25], in which we set the maximum tolerable false alarm probability and maximize the detection probability.

For the proposed EA target detection scheme, the *false alarm (FA) probability* is given by:

$$Q_{FA} = \frac{1}{2}\mathrm{erfc}\left(\frac{t_{sh}}{\sqrt{N_s N_b + (N_s+1)(N_b+1)}}\right), \tag{13}$$

where t_{sh} is the threshold determined from the tolerable FA probability. The complementary error function is defined by $\mathrm{erfc}(x) = (2/\sqrt{\pi})\int_x^{\infty}\exp(-u^2)du$.

On the other hand, the *detection probability* is given by:

$$Q_D = \frac{1}{2}\mathrm{erfc}\left(\frac{t_{sh} - 2\sqrt{TT_i N_s(N_s+1)}}{\sqrt{N_i N_s' + \left(N_i+1\right)\left(N_s'+1\right) - 2TT_i N_s(N_s+1)}}\right). \tag{14}$$

IV. ILLUSTRATIVE NUMERICAL RESULTS

The referent case will be the case in which a coherent state is used to illuminate the target, in the presence of background (thermal) radiation. The density operator, in the presence of thermal radiation, has the following P-representation [1]-[4],[24]:

$$\rho_t = \frac{1}{\pi N_b}\int e^{-\frac{|\alpha-\mu_t|^2}{N_b}}\left|\alpha\right\rangle\left\langle\alpha\right| d^2\alpha, \tag{15}$$

wherein in the absence of the target (t=0) we have that μ_0=0, while in the presence of the target (t=1) μ_1=μ. As before, N_b denotes the average number of thermal (background) photons. The coherent state $|\alpha\rangle$ can be expressed in terms of number states as follows $\left|\alpha\right\rangle = e^{-|\alpha|^2/2}\sum_n(\alpha^n/\sqrt{n!})\left|n\right\rangle$ and after substitution in (15) we obtain:

$$\rho_0 = \sum_{n=0}^{\infty}(1-\nu)\nu^n\left|n\right\rangle\left\langle n\right|, \;\; \nu = N_b/(N_b+1). \tag{16}$$

In the presence of target, the corresponding density matrix can be described as [24]:

$$\left\langle n\left|\rho_1\right|m\right\rangle = \begin{cases} (1-\nu)\sqrt{\dfrac{n!}{m!}}\nu^m\left(\mu^*/\mathscr{C}\right)^{m-n}e^{-(1-\nu)|\mu|^2}\cdot \\ \qquad L_n^{m-n}\left[-(1-\nu)^2\left|\mu\right|^2/\nu\right], \; m \geq n \\ \left\langle m\left|\rho_k\right|n\right\rangle^*, \; m < n \end{cases} \tag{17}$$

where $|\mu\rangle$ is the state used to illuminate the target. In (17), we use $L_d^o(\cdot)$ to denote the associated Laguerre polynomials with subscript d and superscript o denoting the degree and order, respectively. Finding optimum strategy for the Neyman-Pearson criterion would be to determine the eigenvalues η_k and eigenkets $\left|\eta_k\right\rangle$ of the operator $\rho_1 - \Lambda\rho_0$ using the following eigenvalue equation:

$$\left(\rho_1 - \Lambda\rho_0\right)\left|\eta_k\right\rangle = \eta_k\left|\eta_k\right\rangle, \tag{18}$$

wherein the parameter Λ is determined from the maximum tolerable FA probability. This problem has been solved numerically.

To reduce complexity, the *Helstrom threshold detector* can be used [24], with the corresponding detection operator

$$\Pi_{H.t.} = \left(N_b + 0.5\right)^{-1}\left(\hat{a} + \hat{a}^{\dagger}\right) \tag{19}$$

being related to the in-phase operator.

By setting $T=T_i=1$, in Fig. 5 we compare the proposed EA target detection scheme against various coherent states-based schemes, in terms of detection probability vs. signal-to-noise ratio (SNR), for the average number of background photons being $N_b=0.1$ [Fig. 5(a)], $N_b=1$ [Fig. 5(b)], and $N_b=10$ [Fig. 5(c)], wherein the false alarm probability that can be tolerated is set to $Q_{\mathrm{FA}}=10^{-6}$.

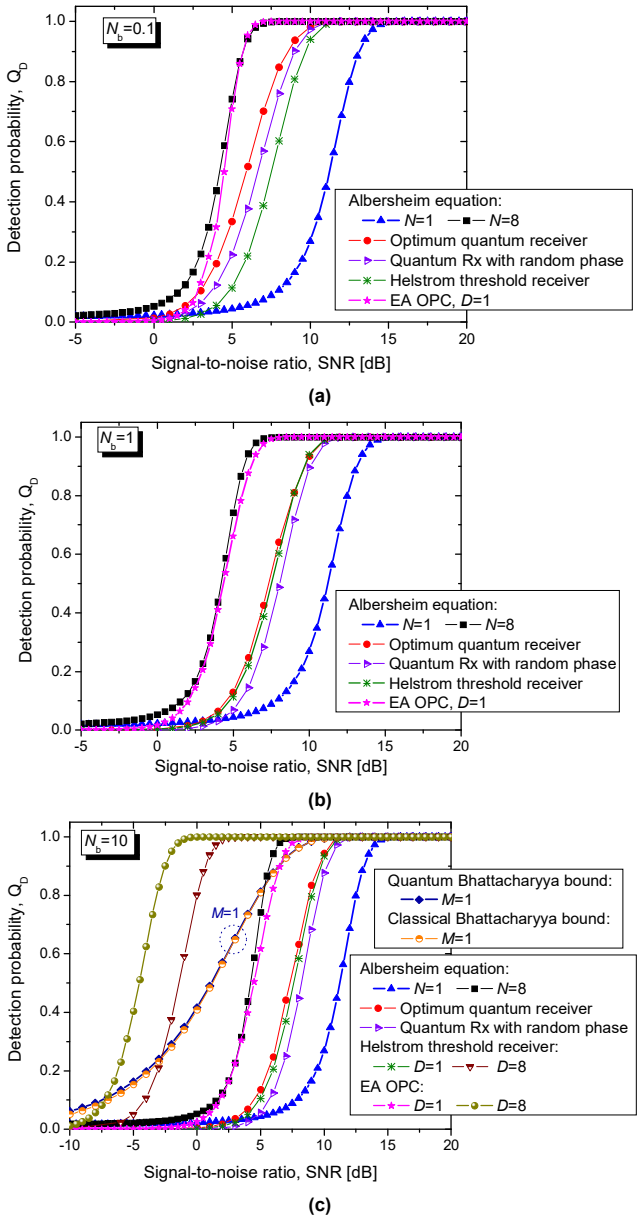

FIGURE 5. Detection probability vs. SNR [dB] for different radar detection schemes for average number of thermal photons being: (a) N_b=0.1, (b) N_b=1, and (c) N_b=10. The maximum tolerable FA probability is set to $Q_{FA}=10^{-6}$. The idler channel is assumed to be ideal (T_i=1 and N_{bi}=0).

The classical Albersheim's equation-based plot is provided as well for the number of samples being $N=1$ and 8 (see refs. [26] and [27] for details related to the Albersheim's equation). The SNR for non-classical target detection schemes is defined by $N_s/(2N_b+1)$. The following three coherent states-based detection schemes are considered: optimum quantum detector, quantum receiver (Rx) in which the phase is random, and Helstrom threshold receiver. Clearly, the proposed EA target detection scheme outperforms various coherent states-based detections schemes and significantly outperforms the classical target detection. As the average number of thermal photons increases, it appears that Helstrom threshold detection scheme performs comparable to the optimum quantum detection scheme, see for instance Fig. 5(b). Another interesting observation is that for $N_b=0.1$ the Helstrom threshold detector performs worse than quantum receiver with random phase, while for $N_b=1$ and 10 it performs better. For $N_b=10$ we also provided both quantum and classical Bhattacharyya bounds, assuming that $M=1$ TMSV state is used, which are strictly speaking tight bounds only in a high-SNR regime.

Given that the SPDC-based entangled source is broadband source in Fig. 5(c) we study the improvement when the number of bosonic modes is increased to $D=8$. The proposed EA target detection scheme significantly outperforms the Helstrom threshold receiver with $D=8$ and classical radar detector for $N=8$. For the detection probability of $Q_{\mathrm{D}}=0.95$ (and false alarm probability of $Q_{\mathrm{FA}}=10^{-6}$), the EA target detection scheme for $D=8$ Bosonic modes outperforms Helstrom detection scheme (also with $D=8$) by 3.12 dB, while at the same time outperforming the corresponding classical scheme with $N=8$ samples by even 8.03 dB.

In Figure 6 we evaluate the EA scheme's detection probability vs. SNR by observing now the Bosonic main (signal) channel model, described by Eq. (7.1). Here we assume the ideal distribution of entanglement over the idler channel ($T_i=1$ and $N_{bi}=0$), while the main channel is considered noisy with parameter N_b being set to 10. Clearly, for low transmissivities of the main channel, the use of single Bosonic mode is not sufficient because the required SNR to achieve high target detection probability is way too high. On the other hand, when eight Bosonic modes are employed, high target detection probabilities are possible even for moderate SNRs when the channel transmissivity is very low.

In Figure 7 we evaluate the proposed EA scheme's detection probability vs. SNR by fixing main (signal) channel transmissivity to $T=0.05$ and varying the transmissivity of the idler channel, with corresponding channel model being described by Eq. (4). Both main (signal) and idler bosonic channels are considered noisy with corresponding parameters being $N_b=10$ and $N_{bi}=2$, respectively. Clearly, when the idler channel is noisy and lossy the same detection probability is achieved for higher SNR values, compared to the case with ideal entanglement distribution. To compensate for this problem, we can increase the number of bosonic modes, which is straightforward to implement thanks to the wideband nature of the SPDC process.

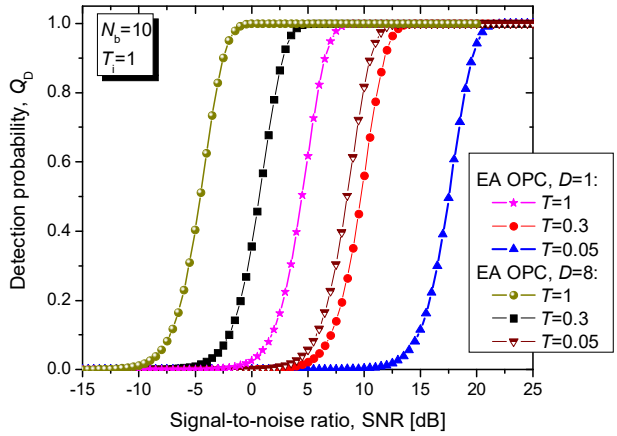

FIGURE 6. **Detection probability vs. SNR [dB] for EA OPC scheme for different main bosonic channel transmissivities. The maximum tolerable false alarm probability is set to Q_{FA}=10^{-6}. The idler channel is assumed to be ideal (T_i=1 and N_{bi}=0).**

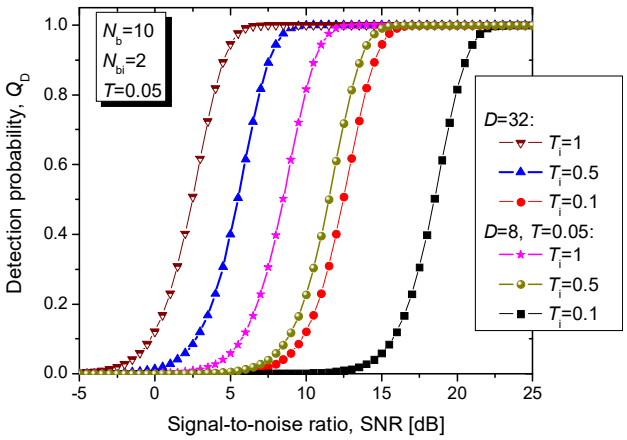

FIGURE 7. **Detection probability vs. SNR [dB] for EA OPC scheme for different idler channel transmissivities. The main (signal) channel transmissivity is set to T=0.05. The maximum tolerable false alarm probability is set to Q_{FA}=10^{-6}.**

V. CONCLUDING REMARKS

In this paper we have been concerned with the entanglement assisted bistatic quantum radar detection. We have proposed the EA radar detection scheme employing the optical phase conjugation on transmitter side and classical coherent detection on receiver side.

The proposed EA target detection scheme has been evaluated against the coherent states-based quantum detection schemes. We have shown that the detection probability of the proposed EA target detection scheme has been significantly better than that of corresponding coherent states-based quantum detection schemes as well as the classical detection. The proposed scheme has been also evaluated by assuming the imperfect distribution of entanglement and by modeling the radar return channel as the lossy and noisy Bosonic channel.

REFERENCES

[1] I. B. Djordjevic, *Quantum Communication, Quantum Networks, and Quantum Sensing*. Elsevier/Academic Press, 2022.

[2] I. B. Djordjevic, *Quantum Information Processing, Quantum Computing, and Quantum Error Correction: An Engineering Approach, 2nd Edition*. London-San Diego: Elsevier/Academic Press, 2021.

[3] G. Cariolaro, *Quantum Communications*. Cham-Heidelberg: Springer International Publishing AG Switzerland, 2015.

[4] I. B. Djordjevic, *Physical-Layer Security and Quantum Key Distribution*. Cham, Switzerland: Springer Nature Switzerland AG, 2019.

[5] S. Guha, B. I. Erkmen, "Gaussian-state quantum-illumination receivers for target detection," *Phys. Rev. A*, vol. 80, no. 5, p. 052310, 2009.

[6] Z. Zhang, Q. Zhuang, "Distributed quantum sensing," *Quantum Sci. Technol.*, vol. 6, no. 4, p. 043001, 2021.

[7] S.-K. Liao *et al.*, "Satellite-to-ground quantum key distribution," *Nature*, vol. 549, p. 43, 2017.

[8] A. S. Holevo, R. F. Werner, "Evaluating capacities of Bosonic Gaussian channels," *Physical Review A*, vol. 63, no. 3, p. 032312, 2001.

[9] H. Shi, Z. Zhang, Q. Zhuang, "Practical route to entanglement-assisted communication over noisy Bosonic channels," *Phys. Rev. Appl.*, vol. 13, no. 3, p. 034029, 2020.

[10] I. B. Djordjevic, "On Entanglement Assisted Classical Optical Communication with Transmitter Side Optical Phase-Conjugation," *IEEE Access*, vol. 9, pp. 168930 - 168936, 22 December 2021.

[11] A. M. Childs, "Secure assisted quantum computation ," *Quantum Information and Computation*, vol. 5, no. 6, pp. 456-466, 2005.

[12] M. Lanzagorta, *Quantum Radar*. Morgan and Claypool Publishers, 2012.

[13] S. Lloyd, "Enhanced Sensitivity of Photodetection via Quantum Illumination," *Science*, vol. 321, no. 5895, pp. 1463-1465, 2008.

[14] J. H. Shapiro, "The Quantum Illumination Story," *IEEE Aerospace and Electronic Systems Magazine*, vol. 35, pp. 8–20, Apr. 2020.

[15] G. Sorelli, N. Treps, F. Grosshans, F. Boust, "Detecting a target with quantum entanglement," arXiv:2005.07116, 2021.

[16] R. G. Torromé, N. B. Bekhti-Winkel, P. Knott, "Introduction to quantum radar," arXiv:2006.14238v3, 2020.

[17] A. Karsa, G. Spedalieri, Q. Zhuang, S. Pirandola, "Quantum illumination with a generic Gaussian source," *Phys. Rev. Research*, vol. 2,no. 2, p. 023414, 2020.

[18] Harris Corporation, *Quantum Sensors Program*, Final Technical Report, AFRL-RI-RS-TR-2009-208, Aug. 2009.

[19] R. Di Candia, H. Yiğitler, G. S. Paraoanu, R. Jäntti, "Two-Way Covert Quantum Communication in the Microwave Regime," *PRX QUANTUM*, vol. 2, p. 020316, 2021.

[20] C. Noh, C. Lee, S.-Y. Lee, "Quantum illumination with definite photon-number entangled states," *J. Opt. Soc. Am. B*, vol. 39, pp. 1316-1322, 2022.

[21] S. Barzanjeh, S. Pirandola, D. Vitali, J. M. Fink, "Microwave quantum illumination using a digital receiver," *Sci. Adv.*, vol. 6, p. eabb0451, 8 May 2020.

[22] S. Hao, H. Shi, W. Li, J. H. Shapiro, Q. Zhuang, Z. Zhang, "Entanglement-assisted communication surpassing the ultimate classical capacity," *Phys. Rev. Lett.*, vol. 126, no. 25, p. 250501, 2021.

[23] Z. Zhang, S. Mouradian, F. N. C. Wong, J. H. Shapiro, "Entanglement-enhanced sensing in a lossy and noisy environment," *Phys. Rev. Lett.*, vol. 114, no. 11, p. 110506, 2015.

[24] C. W. Helstrom, *Quantum Detection and Estimation Theory*. New York: Academic Press, 1976.

[25] R. N. McDonough, A. D. Whalen, *Detection of Signals in Noise*, 2nd Ed. San Diego: Academic Press, 1995.

[26] D. W. Tufts and A. J. Cann, "On Albersheim's Detection Equation," *IEEE Transactions on Aerospace and Electronic Systems*, vol. AES-19, no. 4, pp. 643-646, July 1983.

[27] M. A. Richards, *Fundamentals of Radar Signal Processing*. New York: McGraw-Hill, 2005.

IVAN B. DJORDJEVIC (Fellow, IEEE) is a professor of electrical and computer engineering and optical sciences at the University of Arizona;

director of the Optical Communications Systems Laboratory (OCSL) and Quantum Communications (QuCom) Lab; and co-director of the Signal Processing and Coding Lab. He is both IEEE Fellow and the OSA (Optica) Fellow. He received his PhD degree from the University of Nis, Yugoslavia in 1999.

Professor Djordjevic has authored or co-authored ten books, more than 560 journal and conference publications, and he holds 54 US patents. Dr. Djordjevic serves as an Area Editor/Associate Editor/Member of Editorial Board for the following journals: *IEEE TRANSACTIONS ON COMMUNICATIONS, OPTICA (OSA)/IEEE JOURNAL OF OPTICAL COMMUNICATIONS AND NETWORKING, OPTICAL AND QUANTUM ELECTRONICS,* and *FREQUENZ.* He was serving as editor/senior editor/area editor of *IEEE COMMUNICATIONS LETTERS* from 2012 to 2021. He was serving as editorial board member/associate editor for *IOP JOURNAL OF OPTICS* and *ELSEVIER PHYSICAL COMMUNICATION JOURNAL* both from to 2016 to 2021.

Prior to joining the University of Arizona, Dr. Djordjevic held appointments at University of Bristol and University of the West of England in UK, Tyco Telecommunications in USA, National Technical University of Athens in Greece, and State Telecommunication Company in Yugoslavia.